

Electrical and Joule Heating Capabilities of Multifunctional Coatings based on Recycled Carbon Fiber from Prepreg Scrap

David Martínez-Díaz,* Emma Espeute, Alberto Jiménez-Suárez, and Silvia González Prolongo*



Cite This: *ACS Omega* 2023, 8, 46548–46559

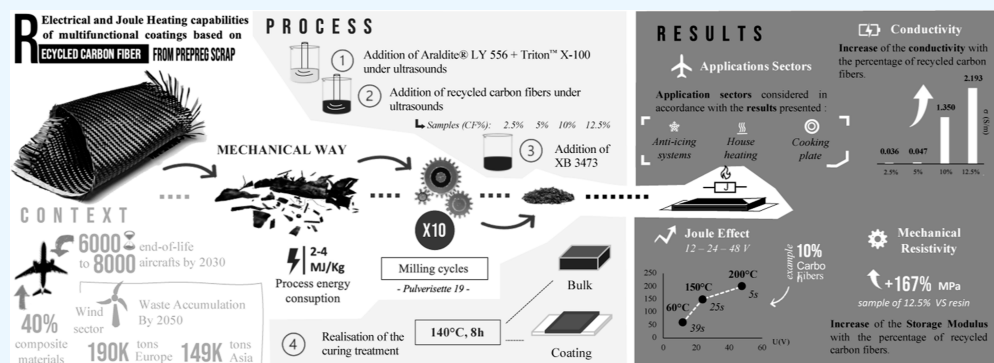


Read Online

ACCESS |

Metrics & More

Article Recommendations



ABSTRACT: The continuous growth in the use of preimpregnated semielaborated products to manufacture continuous carbon fiber-reinforced polymer parts has led the industry to face an important challenge in the management of the prepreg scrap, as the amount of waste produced can reach almost 75% due to the inefficiency of the cutting phase. In this context, this industry is pushed to move toward a circular economy approach by conferring a new use to their waste. The main problem arises from the fact that shortening carbon fiber leads to nonefficient mechanical reinforcement and that other thermal or chemical recycling approaches are environmentally hazardous. In this work, mechanical recycling of carbon fiber prepreps from expired virgin prepreps or scrap from an automated manufacturing operation is proposed as an economical and environmentally efficient method to obtain multifunctional coatings with Joule effect heating capabilities, which are demanded by different industries as a high-value product. As a coating, mechanical performance is not so relevant; nevertheless, obtaining high electrical conductivity by the incorporation of proper size and distributed short recycled carbon fiber can lead to a self-heating coating that could be used for anti- and deicing purposes or any other thermally activated function with very low power consumption. In this way, electrical conductivities up to 2 S/m were obtained, which allowed for achieving temperatures of 200 °C by the Joule effect in all samples in less than 17 s by the application of voltages below 48 V for bulk materials and 100 V for the coating.

1. INTRODUCTION

In the last years, the use of carbon fiber reinforced polymer (CFRP) composites is constantly increasing.¹ An expansion in the European market of 7.5% per year from 2019 to 2025 is expected,² and most of these demands come from the wind energy, aerospace, and automotive industries.³ Normally, this type of composite is used in these industrial sectors due to their high performance, such as high specific stiffness and strength.⁴ CFRP final properties are strongly linked to diverse parameters such as fiber content, orientation, or the selected manufacturing process.^{4,5} In this way, focused on structural parts, the use of preimpregnated fibers, so-called prepreps, is one of the most well-known methods to develop high-performance CFRPs. Parts made from prepreps present unique features, such as high fiber volume content and relatively easy manufacture.⁶ Normally, to achieve better quality parts and higher manufacturing velocities prepreps are combined with

automated processing technologies such as automated fiber placement or automated tape laying, especially in the aerospace industry where high-quality requirements are imposed.^{4,6} At this stage, the volume of production of CFRP has increased along with a corresponding rise in waste generation associated with its manufacturing process. This presents important challenges from both an economic and environmental perspective and underscores the need for sustainable

Received: July 25, 2023
Revised: October 24, 2023
Accepted: October 26, 2023
Published: November 28, 2023



approaches to the production, processing, and reuse of materials.

As previously mentioned, the growing demand for carbon fiber (CF) is associated with some issues related to the relevant environmental impacts of their manufacturing processes.^{7,8} In this way, the development of recovery and recycling systems is highly necessary to recover the residual end-of-life value of these materials.^{9–11} The Directive 2008/98/EC of the European Parliament^{7,9,12} promotes both the prevention of waste production and the reuse and recycling of CFRPs. When prepreps are used, it is interesting to pay special attention to the prevention of waste production, due to their limited shelf life and their manufacturing process. Usually, epoxy prepreps present a shelf life of around 20–40 days at room temperature and 1–2 years at low temperature (–20 °C storage condition), depending on the matrix system and the manufacturer. Moreover, the cutting operations of virgin prepreps roll (as off-cuts, trim waste, or end-roll waste), which are necessary for the CFRP manufacturing process, can constitute between 20 and 70 wt % of the virgin prepreg used.^{9,13–15} Given the substantial volume of prepreg waste generated during the manufacturing of each CFRP part and the high number of parts produced worldwide, this study aims to identify strategies for repurposing this waste into value-added products. Such efforts are particularly important from an economic and environmental perspective, as they can help to minimize waste generation, optimize resource utilization, and promote sustainable materials processing. By developing innovative approaches for repurposing prepreg waste, this study aims to contribute to the advancement of sustainable materials manufacturing and processing practices and support the transition toward a circular economy. For a very long time, landfilling or incinerating have been options for waste management but not the best ones,¹⁶ with negative impacts in terms of environmental impacts and economic costs. Nowadays, there exist three different ways for recycling a CFRP or prepreps:¹⁷ chemical,^{18–20} thermal,^{21,22} and mechanical.²³ From an energy consumption point of view, the last process is the one that consumes the least with a consumption ranging between 2 and 4 MJ/kg.²⁴ Moreover, it is the only technique with no emission of toxic gases, the material can be fed in different forms or geometries and, finally, it is the easiest and cheapest to use.^{17,24} However, this process induces a significant deterioration of different mechanical properties due to the fiber surface damage and shortening of fiber length. Crushing impairs the CF properties, such as their mechanical resistance.^{25,26} Recycled fibers are short in comparison to the originals, and by this fact are assumed to be less effective than long fibers from a mechanical point of view.^{17,27} As a result, the short fibers obtained from mechanical recycling are typically unsuitable for use in the production of structural components, although short CF can provide an increase in mechanical strength when used as reinforcement of polymeric matrices, both thermosetting and thermoplastic. On the contrary, it must be pointed out that the other recycling methods (chemical or thermal) ideally can recover the long fibers and, therefore, ideally could be reused in applications that involve high mechanical resistance.

This work is focused on the mechanical recycling process of CF-epoxy prepreps. The specific conditions related to the use of prepreps for the manufacturing of CFRP composites, previously detailed, entail the presence of tons of waste derived from the manufacturing process, even before the end-of-life of

the composite. So, it is an interesting material to recycle, thus avoiding its arrival at landfills and significantly improving the management of this waste. More specifically, the aim of the present work consists of the development of new multifunctional materials by using the obtained recycled short CF as reinforcement of a polymeric matrix to mainly improve their mechanical, thermal, and electrical properties and confer new multifunctionalities to the original polymeric matrix. As previously suggested, considering the probable impaired mechanical behavior of these new composites reinforced with short CF in bulk with regard to the long fiber reinforced ones, these materials were also manufactured as functional coatings for which the mechanical performance in terms of stiffness and strength is not so important. Using the obtained short CF as reinforcement in coatings seems an interesting application to take advantage of not only the common protective properties sought by coatings (such as chemical and abrasion protection) but also new functionalities over the substrates. Integrating different functions in one material system is a challenge, especially if those functions seem to exclude each other²⁸ (i.e., polymer with high electrical conductivities). Understanding function-structure relationships and developing a competence in the system approach for multifunctionality enables many modern applications, which can improve quality of life and address important global challenges.²⁸ In this case, taking into account the used material (epoxy matrix and recycled CFs) multifunctionality can be reached by combining the barrier behavior (from the epoxy matrix) or the wear resistance (from the CF) with new functionalities/applications such as surface heaters for anti-icing and deicing surfaces^{29,30} and heating devices.^{31,32} To achieve optimal performance in these applications, it is common to use carbon fillers.²⁸ Using carbon nanotubes (CNT) moderate heating up to 150 °C can be achieved through the joule effect at low voltages (25–100 V).^{33,34} Another alternative is the use of graphene nanoplatelets (GNP), which can achieve higher temperatures but also require higher voltages (180 °C at 150 V).³⁵ CFs were also used for these applications being the most common practice the use of a virgin continuous reinforcement, instance of short fibers, achieving temperatures exceeding 200 °C even with voltages below 10 V.³⁶ Other interesting new functionalities/applications for this type of fillers can be electromagnetic shielding,^{37,38} lightning protection,^{39,40} and antistatic electrical conductors surfaces,⁴¹ among others.²⁸

Thus, the goal of this study is to explore sustainable approaches for the management of waste generated by the use of prepreps in the manufacture of CFRP. The study aims to identify alternatives that are environmentally sound, economically viable, and technically feasible. To this end, mechanical recycling has been investigated as a potential solution, and the recycled material has been utilized in two distinct applications: as a bulk material and as coatings. As a functional coating, the high-value obtained product can give a second opportunity to the recycled carbon fibers as the mechanical requirements are no longer required, thus allowing a shortening effect during mechanical recycling. To achieve this goal, first, the effect of the milling cycle on the recycled product has been analyzed. Subsequently, the impact of adding different amounts of recycled short CF to a polymeric matrix was evaluated in terms of changes in its mechanical, electrical, and thermoelectric properties.

2. EXPERIMENTAL SECTION

2.1. Materials. The study aims to develop multifunctional materials, bulks, and coatings based on the combination of a polymeric matrix with a carbon fiber reinforcement achieved from the mechanical recycling of expired prepregs. The selected matrix for the fabrication of the samples was the Araldite LY 556, a Bisphenol-A-based epoxy resin, and the XB 3473, a polyamine-based hardener, provided by Huntsmañs industry. The carbon fiber epoxy prepregs used to obtain short carbon fibers by a milling process were obtained from an expired virgin prepreg roll and manufacturing cutting process. Moreover, Triton X-100, purchased from Sigma-Aldrich, was used as a surfactant to achieve a better dispersion of the milled carbon fibers on the LY 566/XB 3473 epoxy system. All chemicals were used as received without further purification. Finally, glass fiber-epoxy laminate Durostone EPC 203, provided by Röchling Composites, was used as a substrate for the application of the developed coatings. Moreover, Loctite EA 9466 was used as the adhesive to evaluate the adhesion resistance of the applied coatings.

2.2. Sample Preparation. As previously detailed, the aim of the study is to develop multifunctional materials based on the combination of the reinforcement of a polymeric matrix with carbon fibers achieved from the mechanical recycling of expired prepregs. The milling of the expired prepregs used for the recycling process was carried out with a Universal Cutting Mill PULVERISETTE 19 with a speed revolution of 3000 rpm. The mill was equipped with a disk milling cutter rotor with fixed knives made of hard metal tungsten carbide and a recuperation sieve cassette of 2 mm with trapezoidal perforation. The utilization of an inferior speed causes poor fiber milling and an accumulation of noncrushed fibers inside the machine. A total of 10 milling cycles were used for each recycled material batch to ensure a homogeneous fiber length, allowing increasing the process's reproducibility. Details about the obtained product are reported in Section 3.1. Different CF contents, between 2.5 and 12.5 wt %, were mixed with the epoxy resin to generate new composite materials and evaluate their influence on the mechanical, electrical, and thermo-electrical properties of the synthesized composites. For a better dispersion of the CF, avoiding the presence of agglomerates, a nonionic surfactant, Triton X-100, was used in a proportion of 5 wt %. The surfactant was manually mixed with the epoxy monomer (LY 566), and, after the incorporation of the carbon fibers, the mixture was left under ultrasound by means of a sonication horn for 15 min until the CFs were fully dispersed and homogeneously incorporated into the monomer. The mixture was degassed by a vacuum pump before and after the incorporation of the CFs to eliminate the air contained inside of the mixture, 15 min each cycle, avoiding the presence of porosity on the final composite. After the second degasification step, the hardener (XB 3473), was incorporated into the mixture and then poured into a mold or applied as a coating. The epoxy system LY 556 and XB 3473 were mixed in the following mass proportions, 100:23. For the preparation of the coating samples, a special rectangular metal film applicator with a width of 100 mm and a 1 mm thickness gap was used at a constant speed of $1.5 \text{ mm}\cdot\text{s}^{-1}$. Glass fiber-epoxy laminates were used as substrates for the application of the coatings. Finally, all samples, bulks, and coatings, were cured at $140 \text{ }^\circ\text{C}$ for 8 h in a convection oven to allow the reticulation and the formation of a cross-linked resin.

2.3. Characterization. Different characterization techniques were carried out to analyze the samples before and after composite manufacturing. First, it was necessary to characterize the obtained carbon fibers from the different milling cycles applied. Then, different characterization techniques were used to analyze the performance of the new upcycling materials, which were presented in two different morphologies: bulk and coatings.

Optical microscopy (Leica DMR) is used to analyze the size distribution of the obtained carbon fibers after the milling process. Samples were prepared by dispersing a few grams of fibers in a tetrahydrofuran (THF) solution and then dropping a few drops of this suspension in a small glass. Using optical microscopy measurements were made with $\times 5$ and $\times 10$ lenses, and subsequently, the Leica Application Suite software was used to determine the length of the fibers. Despite using two different lenses, the same area was analyzed with both lenses and different fiber length ranges were evaluated with each one, with the aim of not duplicating measures during the process. A thermogravimetric analyzer TGA from Mettler Toledo was used to determine the mass loss of the recycled fibers during a heating cycle up to $800 \text{ }^\circ\text{C}$. In this way, the remaining prepreg matrix content in the samples after the different milling cycles carried out can be evaluated, thus analyzing the matrix-fiber separation on the recycled product after the milling process.

A Hitachi S-2100N scanning electron microscope (SEM) was used to analyze the obtained milled carbon fibers, the cross-sectional view, and the fracture surface of the manufactured composites. Additionally, a field emission gun-SEM (FEGSEM) Nove NanoSEM FEI 230 was also used to acquire images at higher magnification and resolutions.

Thermomechanical properties of the manufactured composites were characterized by dynamical mechanical thermal analysis (DMTA) performed on bulk samples thanks to Q800 equipment supplied by TA Instruments. This equipment allows to evaluate the storage modulus (\dot{E}) and the glass transition temperature (T_g), the last one obtained from the peak of the $\tan \delta$ curve. DMTA tests were performed according to the ASTM 5418 standard in the dynamic single cantilever mode at 1 Hz for $35.0 \text{ mm} \times 12.0 \text{ mm} \times 1.7 \text{ mm}$ specimens with a temperature range from 30 to $200 \text{ }^\circ\text{C}$ at $2 \text{ }^\circ\text{C}/\text{min}$ speed.

Electrical conductivity is measured by a Keithley-2410 source meter instrument on bulks and coatings. Five different voltages (U) were applied between 0 and 20 V with a current (I) limit of 1 A, at room temperature. Bulk samples were prepared with dimensions of $10 \times 10 \times 1 \text{ mm}$, while coating presents dimensions of $100 \times 50 \text{ mm}$ over the glass fiber substrates. The calculation of the electrical conductivity (σ) is carried out according to an approximation based on Oh's law supposing a linear response of the current as a function of the voltage. For the bulk samples, the distance between electrodes was 10 mm, while in the case of using coatings, the distance between electrodes was 50 mm.

Using Oh's law, the collected values allow the extraction of the electric resistance (R), expressed in ohms (Ω), from eq 1. The electrical conductivity (σ) measured in $\text{S}\cdot\text{m}^{-1}$ is obtained from eq 2, where L (m) represents the distance traveled by the electrons across the sample and A (m^2) represents the cross-section of the sample. Finally, the resistivity (ρ), measured in $\Omega\cdot\text{m}$, is obtained as the inverse of the electrical conductivity (eq 3). Results are obtained from the linear assumption of the

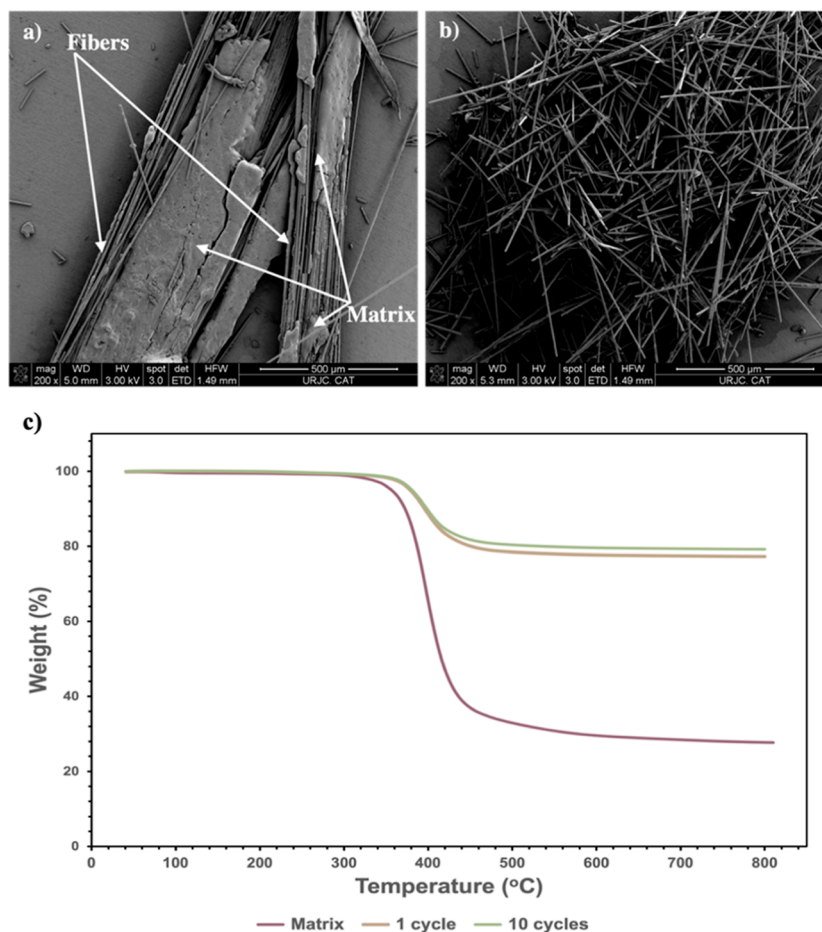


Figure 1. FEGSEM images of the obtained carbon fibers after 1 (a) and 10 (b) milling cycles. (c) TGA thermogram of the polymeric matrix and the obtained milled products after 1 and 10 cycles.

I – V relation, so resistivity and conductivity are average values obtained according to eqs 1–3.

$$I = \frac{U}{R} \quad (1)$$

$$\sigma = \frac{L}{R \cdot A} \quad (2)$$

$$\rho = \frac{1}{\sigma} \quad (3)$$

The Joule effect is measured by a current source meter (Keithley 2410) combined with a thermal camera (FLIR E50). The measures are performed on standard voltages of 12, 24, and 48 V. It is important to point out that to avoid the possible thermal degradation of the samples (bulks and coatings), a limit of 200 °C is established, as it is considered that higher temperatures might degrade the polymer matrix. Moreover, a pull-out adhesion tester PosiTest AT-A was used to determine whether the joule effect heating implies changes in the adhesion properties of the coating. Adhesion tests were performed on coatings, before and after the Joule effect heating, using Loctite EA 9466 as adhesive and dollies with 10 mm of diameter.

3. RESULTS AND DISCUSSION

3.1. Study of Milled Carbon Fibers. Milling processes normally present great difficulties to obtain a homogeneous

product, being necessary to carry out the process more than once.² In this work, 10 milling cycles were performed to achieve homogeneity of the obtained carbon fibers (CF). In order to analyze the morphology variation of the milled product, FEGSEM images after the first and tenth milling cycles were acquired (Figure 1a,b, respectively). As can be seen, large pieces of a polymeric matrix with carbon fibers inside were obtained in a single milling cycle (Figure 1a). This morphology noticeably changes after 10 cycles (Figure 1b), where individual fibers can be seen without a polymeric matrix presence. Taking into account that the objective of this work is the use of recycled milled CF as reinforcement of a new polymeric matrix, the presence of individual fibers ensures better integration of the recycled material on the epoxy resin. Moreover, due to the use of a cutting mill the fiber surface does not appear to be damaged, remaining straight and smooth until the cut region. The reduction of the polymeric matrix content on the milled CF was also analyzed by thermogravimetric analysis (Figure 1c). First, the original epoxy matrix obtained from the expired prepregs was analyzed, observing a large reduction in mass from 350 °C; this drop is related to the thermal degradation suffered by this type of polymeric material. On the contrary, this pronounced drop at 350 °C was not observed with the measured recycled CF samples after 1 or 10 milling cycles, indicating a low presence of the original expired resin in both samples. In addition, the weight loss observed with the milled prepreg samples after the first cycle is 4% higher than that obtained after ten cycles. So, by increasing

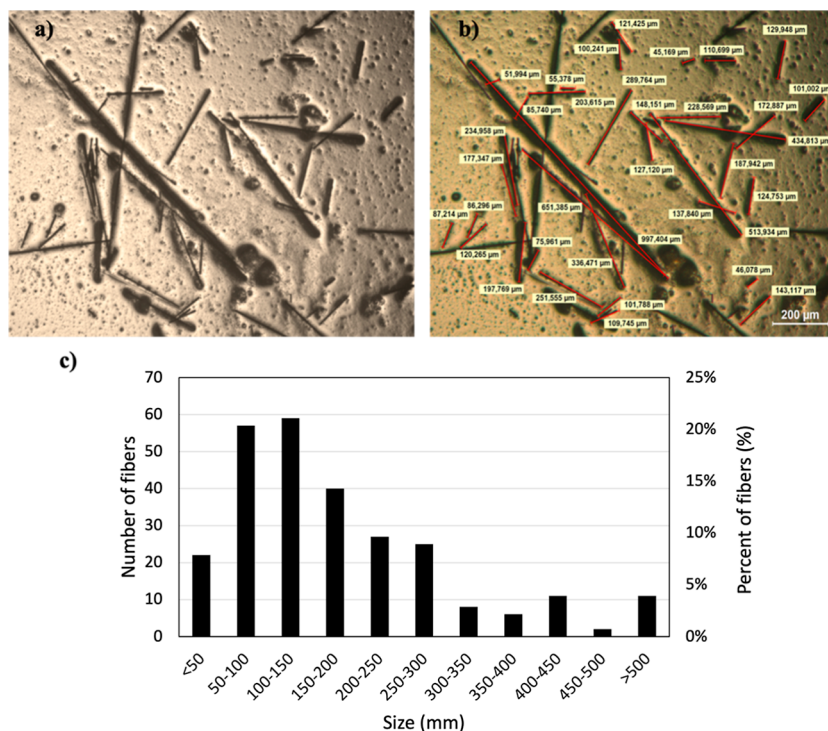


Figure 2. Optical micrographs at 50 \times magnification of the milled carbon fiber without (a) and with (b) the measured length. Milled carbon fiber length size distribution (c).

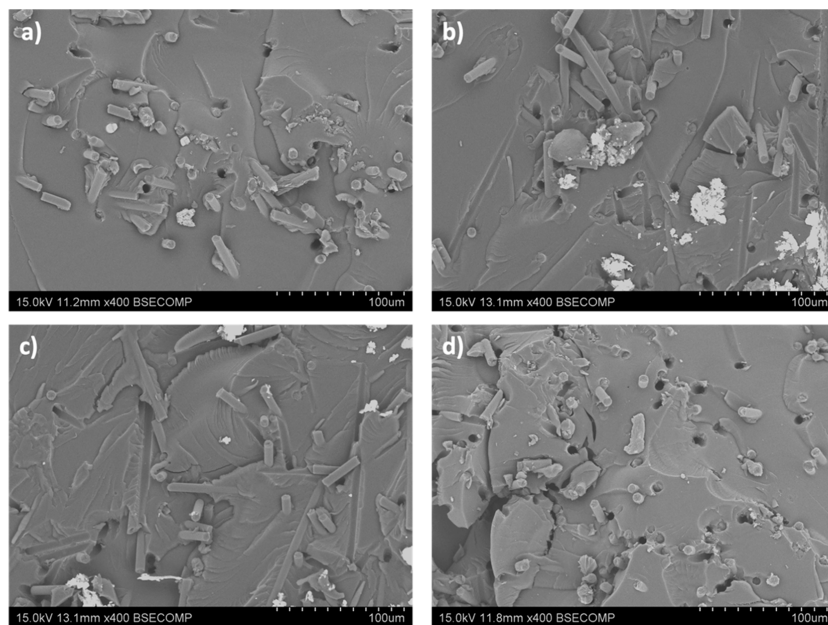


Figure 3. SEM cross-sectional views of the synthesized composites with different carbon fiber contents: 2.5 (a), 5 (b), 10 (c), and 12.5 wt % (d).

the number of cycles, it is possible to reduce the presence of the original epoxy matrix from the expired prepregs. This result is coherent with the previous evaluation of FEGSEM images.

The polydispersity of the final obtained milled CF was analyzed from more than 250 specimens that are counted and measured with an optical microscope. Figure 2 shows a representative example of the obtained carbon fibers without and with the measured fiber length (Figure 2a,b, respectively). Analyzing the results, the highest populations were observed for the length range of 100–150, 50–100, and 150–200 μm , in this order. The sum of the fibers of these lengths represents

60% of the total fibers. The amount of fiber with lengths between 200 and 300 μm represents 20% of the fibers, while fibers longer than 300 μm represent 14%. Regarding the shortest fraction, less than 50 μm , these represent 8% of the fibers. Figure 2c summarizes the obtained results for the polydispersity study.

3.2. Characterization of Composites. **3.2.1. Morphology.** In this section, the morphology of the fracture surface of the different synthesized composite materials is analyzed to verify the distribution of the fiber in the matrix as well as the matrix-reinforcement interface. All fractures were performed by

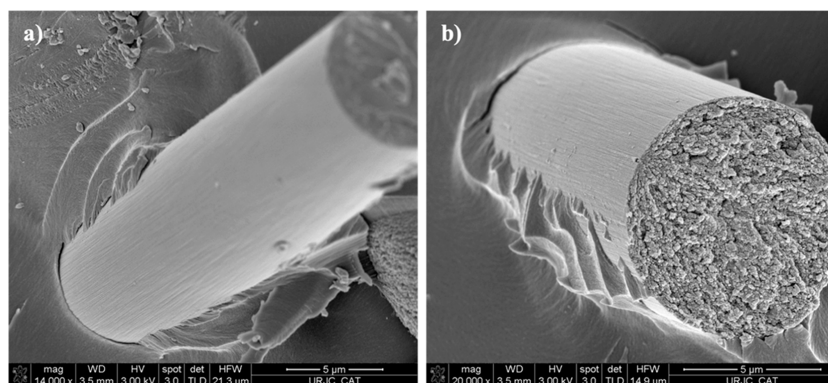


Figure 4. (a, b) Fracture surface by FEGSEM.

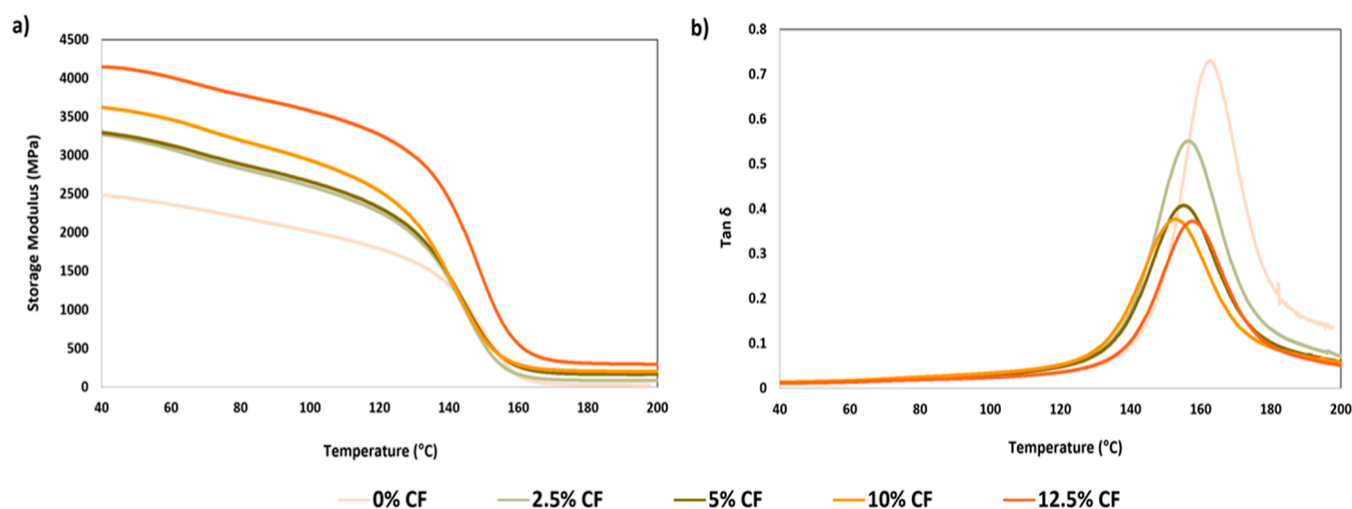


Figure 5. Storage modulus (a) and Tan delta (b) as a function of the temperature and carbon fiber content.

submerging the bulk in liquid nitrogen to obtain a flat fracture surface for the analysis by SEM and FEGSEM. Figure 3 collected four SEM images of the fracture surface obtained by cryogenic fracture of a bulk sample from each manufactured CF content. In all cases, a random orientation of the fibers was achieved but a more uniform distribution in the thickness of the bulk is achieved when the CF content increases. This is related to the fact that an increase in the CF content implies an increase in the viscosity of the resin, which allows the achieved dispersion to be more stable, reducing the reaggregation and the sedimentation effects. Regarding the fracture surface, ductile and brittle fractures refer to the way a material breaks under stress. Ductile fractures occur when a material deforms before breaking, while brittle fractures occur when a material breaks without significant deformation. Many epoxy resins usually show brittle fracture behavior with smooth fracture surfaces, very low plastic deformation, and typical cleavage marks. This is particularly common in epoxy resin with higher T_g ⁴² which is the case of the LY556/XB3473 system. While the addition of the CF can make the material more brittle. This is because the carbon fibers do not deform significantly under loads and thus do not contribute to the plastic deformation of the composite material. CFs can contribute to an increase of other mechanical properties (discussed in the next section), but they can activate different energy consumption processes during fracture, such as crack deviation through the interface, pull-out of fibers, and so forth. In this way, composites with

low CF content, 2.5 and 5 wt % (Figure 3a,b, respectively), presented smoother surfaces with large fracture areas without significant plastic deformation which may be related to a more brittle behavior.⁴³ On the contrary, a different fracture surface can be seen with the highest contents of CFs, 10 and 12.5 wt % (Figure 3c,d, respectively). In these cases, due to the higher presence of fibers, the composites show more complex fracture surfaces with several different fracture planes as a result of crack deviation during its propagation, associated with the presence of the fibers. A deeper analysis of the interface region will shed light on some of the energy consumption mechanisms during fracture. At the maximum content tested, 12.5 wt % (Figure 4d) some small cracks can be easily observed in the resin matrix. This effect has been previously referred to by other researchers as the consequence of lots of fibers pulled out from the polymer matrix in different directions during fracture.⁴² Besides, the interface between matrix and carbon fiber can be improved through the chemical reaction between the partially cured resin surrounding the fibers and the polymer matrix, which could lead to improved interfacial adhesion in the coating. This improved interfacial adhesion between polymer and reinforcement through chemical interaction in coatings has been observed by other authors in polymer coatings with different carbon-based reinforcements such as CNF/MXene or graphene oxide.^{44,45}

Higher magnification analysis of areas surrounding the fibers reveals a good interface between the fiber and matrix. Figure 4

shows two examples of matrix fibrillation during fiber pull-out, which was observed as one of the main strengthening mechanisms in Figure 3. Figure 4a seems to be a fractured fiber, which would mean that in addition to the pull-out effect, some fibers have a good interface and break before detaching from the matrix. Although the fracture could be also associated with the initial milling step of fibers, Figure 4b shows important deformation in the matrix region at the interface, and the fiber is surrounded by the epoxy resin on the lower side until the front of the fiber, which would be probably associated with a fiber breakage after impregnation, that is, during the material fracture. Analyzing both Figure 4a,b, it can also be seen how the fiber surface does not seem damaged by the recycling process, despite having been introduced as reinforcement in the matrix. All these aspects allow concluding that the addition of the recycled CFs activates several mechanisms during fracture such as pull-out and fiber breakage that in turn would translate into a possible increase of energy consumption during fracture and reveals a very good adhesion between resin and recycled CFs. To summarize this section, although Figure 3 reveals a pull-out effect with the remaining holes in the resin when fibers are extracted, Figure 4 shows two important effects: the good integrity of the fiber surface even after the milling process and manufacturing of the composite (Figure 4a) and the energy consumption mechanisms activated in the resin during the fracture process, as fibrillation of the resin is observed clearly in Figure 4b. This fibrillation of deformation during fracture of the brittle resin can be attributed to good interface during the pull-out of the fibers.

3.2.2. Thermomechanical Properties. In order to analyze the effect on the thermomechanical properties of the different CF amounts used as reinforcement, Figure 5 shows the obtained results from the DMTA tests. The percentages of reinforcements used were 2.5, 5, 10, and 12.5 wt % of the previously milled CF. It has to be pointed out that, despite using a surfactant and the long sonication times, reinforcement percentages higher than 12.5 wt % could not be used due to the presence of agglomerates in the epoxy matrix and its unprocessable viscosity. It is important to note that Triton X-100 was added as a surfactant even in the samples without CFs where its use would not be necessary, but in this way, the same methodology was maintained in all samples, allowing analysis of only the effect of the CF content.

The storage modulus of the composites is higher than that of the pure system (Figure 5a). In all cases, the storage modulus value slowly decreases with the temperature until proximally 100 °C, then the \dot{E} rapidly decreases around 85% at 160 °C. Analyzing the CF content effect, the higher content implies a higher value in all the studied temperature ranges. A storage modulus of 2488 MPa was obtained at 40 °C with the sample without a carbon fiber reinforcement. An increase of around 32% in the mechanical properties was obtained in the case of using 2.5 and 5 wt %. Better results were obtained when 10 and 12.5 wt % of CF were used, where improvements in the storage modulus of 46 and 66% were achieved, respectively. While milled CFs have shown potential in improving the mechanical properties of manufactured composite materials, it is important to note that such reinforcement is not typically pursued with the primary aim of enhancing mechanical performance with thermoset polymers. Rather, the addition of milled CF is often intended to provide other benefits, such as improvements in thermal or electrical conductivity as well as increased resistance to fracture or deformation under specific loading conditions.

Furthermore, the use of recycled CF as a reinforcement also presents significant environmental benefits. The utilization of these recycled fibers contributes to waste elimination and management while simultaneously reducing the need for additional fiber manufacturing, which is a recourse-intensive process. These benefits align with broader sustainability objectives in materials science and engineering and highlight the potential for recycling initiatives to support the development of environmentally conscious composites.

On the other hand, the T_g of the specimens (Figure 5b), measured as the maximum of $\tan \delta$ peak, decreases when the CF content increase. Lower and wider $\tan \delta$ peaks were obtained as a consequence of the CF presence in the polymeric matrix, which reduce the cross-link density possibly due to the steric hindrance caused during the curing process. The highest T_g was achieved for the neat sample without CF, this value was 163 °C. Increasing the CF content to 2.5, 5, and 10 wt % the T_g value slightly decreases until up to 153 °C (4–6% drops). These results can be explained by the presence of short fibers in the epoxy matrix, which could hinder the curing reaction of the network. In the case of using 12.5% CF as reinforcement, a different trend was observed because the T_g value slightly increased with respect to the previous results. The obtained result with 12.5 wt % samples are 3% higher than that observed with the 10 wt % of CF, but still lower than the samples without CF (3% lower). This slight increase in T_g value may be related to the large increase observed in the mechanical properties and the DMTA method itself, which relates the T_g values to the flexural behavior of the samples. At high reinforcement contents, they are usually agglomerates, reducing their effective specific area and therefore decreasing their negative effect on the curing process.

Additionally, only one peak can be observed on the $\tan \delta$ representation (Figure 5b) despite using CF obtained from the mechanical recycling of expired epoxy carbon fiber prepreps. Due to the original prepreg resin being completely outdated, it has been observed that the resin is prone to separation from the fibers during the milling process. Consequently, the final composite contains a negligible amount of the old resin compared with the amount of new resin present in the material. Thus, just one T_g was obtained for each material despite the use of different CF contents. Moreover, if the old resin is still activated, then it is perfectly miscible with the new one, both epoxy-based, justifying, in the same way, the observation of a single peak on the $\tan \delta$ representation. This last fact could not have been observed if the recycled CF was obtained from a used CFRP piece, where the resin is strongly bonded to the fiber due to the cross-linking process related to the curing step of the composite.

3.2.3. Electrical Conductivity. The electrical conductivity of the synthesized bulks was analyzed from 0 to 20 V, using Ohm's law. An increase in carbon fiber content corresponds to an increase in conductivity, due to the greater presence of conductive paths. 0.33 and 0.54 $S \cdot m^{-1}$ were achieved for the samples with low carbon fiber content, 2.5 and 5%, respectively. Higher values were obtained with 10 and 12.5% CF, where conductivities of 1.92 and 2.08 $S \cdot m^{-1}$ were obtained, respectively. Table 1 includes a comparison of the presented results in this study with other experimental data reported in available literature for a wide variety of epoxy matrix reinforced with other carbon fillers such as carbon nanotubes (CNT), graphene nanoplatelets (GNP), carbon black particles (CB), or carbon fibers (CF). First, note that the

Table 1. State-of-the-Art in Electrical Conductivity of Epoxy Matrix with Carbon Particle Reinforcements

filler type	filler amount (wt %)	electrical conductivity (S/m)	ref.
CNT	0.5	1.11×10^{-2}	46
CNT	0.5	1.20×10^{-5}	47
CNT	2.0	7.90×10^{-5}	47
CNT	0.7	6.00×10^{-3}	48
CNT	2.0	7.50×10^{-3}	49
CNT	5.0	4.75×10^{-2}	49
GNP	1.0	2.60×10^{-6}	50
GNP	2.0	3.10×10^{-4}	50
GNP	8.0	4.00×10^{-3}	31
CB	40.0	1.40×10^{-8}	51
CB	70.0	1.00×10^{-4}	51
CB	1.2	6.30×10^{-4}	52
CF	10.0	1.00×10^{-4}	53
CF	2.0	2.00×10^{-3}	54
CF	2.5	3.30×10^{-1}	this work
CF	5.0	5.40×10^{-1}	this work
CF	10.0	1.92	this work
CF	12.5	2.08	this work

large difference in the filler amount that can be used with each filler type, for the composite manufacturing process itself, clearly increases the complexity of a rigorous comparison. In general, the use of CB implies the need to use the largest filler amounts. Nevertheless, these epoxy materials with a CB presented the lowest electrical conductivities. On the other hand, using GNP higher electrical conductivities can be achieved, despite using less filler content. The best results were observed when the epoxy matrices are reinforced with CNT, achieving higher conductivities with smaller filler amounts (with respect to CB and GNP). These good results also justify the large number of scientific publications on the subject focused on the improvement of the electrical conductivity of polymeric matrices by using CNTs. Anyway, the electrical conductivities achieved when the milled carbon fibers, obtained from an expired prepreg, were used as fillers were significantly higher than those observed with the other carbon fillers previously mentioned.

3.2.4. Joule Effect Heating. The results of Joule effect heating on bulk samples are represented in Figure 6, and experiments with all carbon fiber contents were performed at 12, 24, and 48 V. In all cases, tests were stopped at 30 s or if the temperature sample achieved 200 °C, to avoid degradation problems. First, it must be pointed out that no temperature

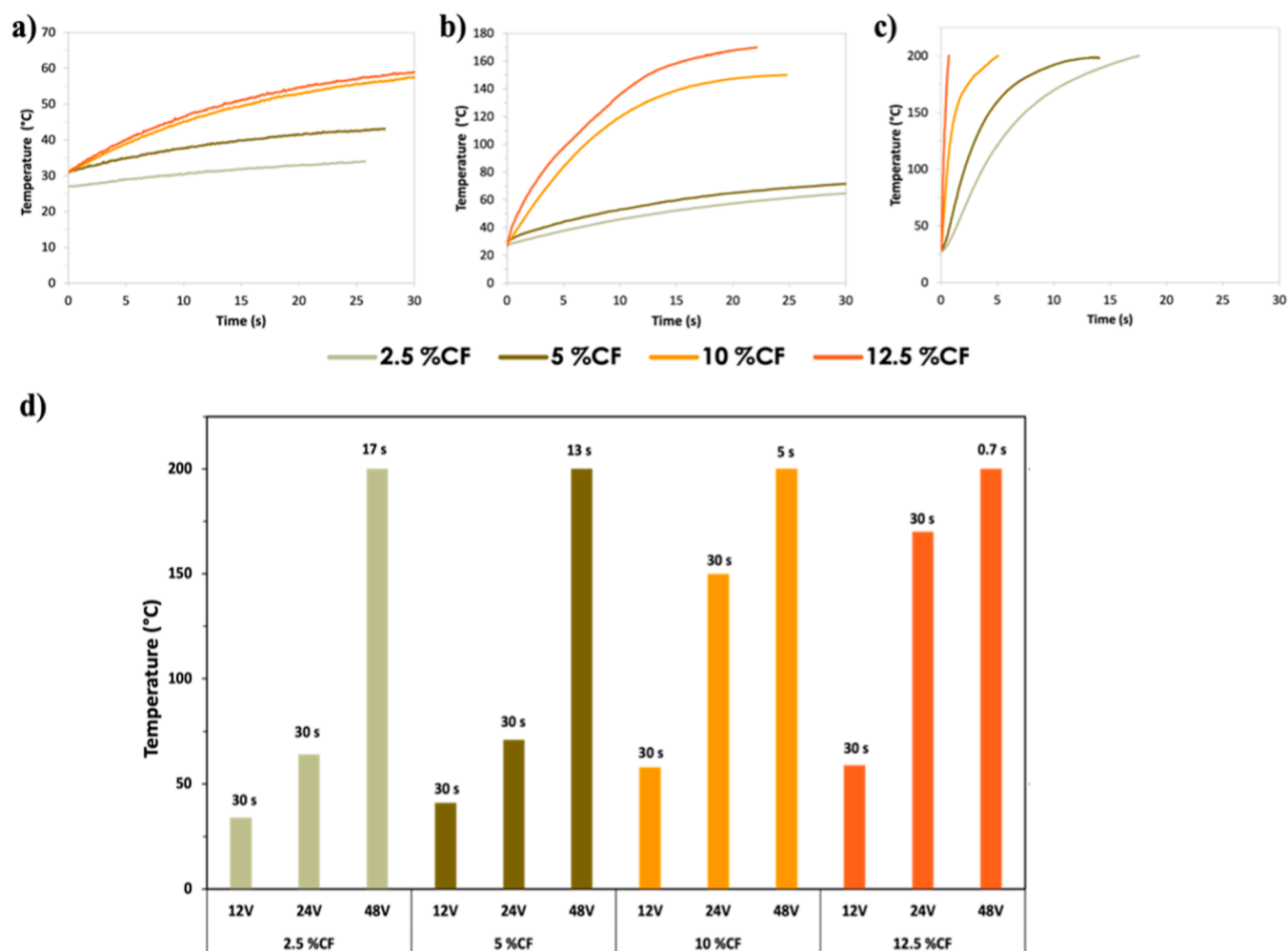


Figure 6. Joule effect of composites as a function of carbon fiber content applying 12 (a), 24 (b), and 48 V (c). (d) Representations of the highest temperature values applying 12, 24, and 48 V, and the time (s) needed to reach it, according to the temperature ranges required for each application.

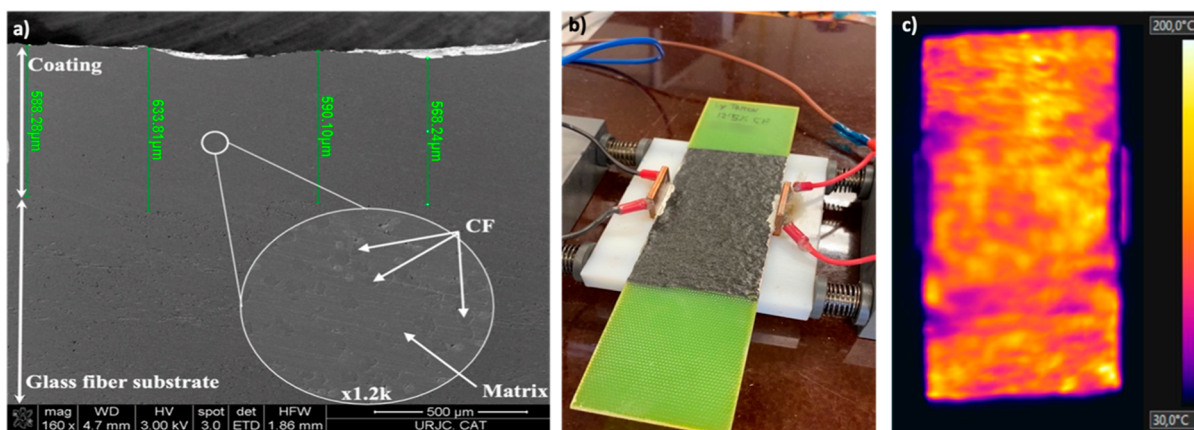


Figure 7. (a) Cross-sectional view of the applied coating on a glass fiber composite substrate. Experimental setup (b) and Joule effect of the coating with 12.5% CF content at 100 V after 120 s (c).

increase was observed with the samples without carbon fiber reinforcement. On the contrary, the Joule effect was observed for the other materials with CF. In a general way, a greater amount of carbon fibers as reinforcement and/or a higher applied voltage on the synthesized materials implies greater and faster heating.

Using 12 V (Figure 6a) small heating was obtained for the 2.5% CF samples, achieving a homogeneous average temperature sample of 34 °C. Higher heating was obtained with the other CF content; temperatures of 42, 58, and 59 °C were achieved for the 5, 10, and 12.5% contents, respectively. Better results were observed in all cases with the 24 V experiments (Figure 6b), obtaining higher temperatures more quickly. The achieved temperatures were 64, 71, 150, and 170 °C, from 2.5 to 12.5% of CF. Finally, using 48 V (Figure 6c) all experiments were stopped because 200 °C was achieved with all of the CF contents. Otherwise, significant differences were observed in the time required to reach that temperature being necessary 17 s for the 2.5% CF samples and just 1 s for the 12.5% CF contents. These results represent a significant improvement in comparison with the reinforcement of epoxy resins with graphene nanoplatelets (GNPs) or carbon nanotubes (CNTs) where higher voltages were required to obtain lower and slower Joule effect heating. For example, looking for the ice-prevention and deicing capacity by using CNTs and graphite (separated and combined) as reinforcement, some authors did not observe temperature increases above 66 °C despite working in higher voltage ranges from 50 to 300 V.⁵⁵ Another example where the same application was also searched in the case of the use of a 10 wt % of GNP, but this case required an application of 250 V to achieve a temperature sample of only 100 °C.³¹ On the other hand, by using GNPs and CNTs until 12 wt % (separated and combined) some authors were able to observe heating due to the Joule effect at low voltages, specifically using 12 V (as in this work), but in their case only heating up to 43 °C was achieved.⁵⁶ In addition to the better performance shown through the use of recycled fibers from expired preregs, it is important to note that unlike the reinforcement used in this work, none of the materials mentioned above are recycled materials.

Figure 6d represents the maximum temperatures reached by joule effect applying 12, 24, and 48 V considering the previously mentioned experiment limits. These limits refer to the fact that the reached temperature was taken after 30 s, or if the sample reaches 200 °C in less than 30 s, the necessary time

to reach said temperature will be recorded. Moreover, Figure 6d also represents the necessary temperature range to be able to use these synthesized materials in different fields. The 3 selected fields are house heating (20–100 °C), anti-icing surfaces (60–80 °C), and hot food-keeping devices (50–200 °C). As can be seen in Figure 6d, the obtained results support the idea that composite materials obtained from CF upcycling can be applied in industrial and domestic applications for standard application voltages (200–240 V), but with low energy consumption, because they can be used with low voltages as low as 12, 24, or 48 V.

3.3. Application as Coatings. Given the good results obtained with the bulk samples, coatings with the epoxy matrix with 12.5% CF were applied over epoxy-glass fiber composite substrates. Furthermore, as previously detailed, the use of discontinuous reinforcements (such as the milled CF used in this work) is not typically pursued with the primary aim of enhancing the mechanical performance to match it with the use of continuous reinforcement, which would be unachievable. Therefore, it has been thought that the use of these materials as coatings, where the mechanical properties are not as demanding as that of structural parts, can be a viable and interesting application at the industrial level for the materials presented in this work. In order to generate the coating samples, after the incorporation of the CF on the epoxy matrix, the mixture was poured at room temperature on the fiberglass composite surface and slowly applied at 1.5 mm·s⁻¹ with a film applicator device. After that, the resin was cured in the same way as that of the bulk samples. The cross-sectional view of a manufactured coating on the glass fiber substrate is collected in Figure 7a. As can be seen, the coating presents good continuity with a homogeneous thickness of around 600 μm. Due to the absence of porosity or delaminated areas, it is difficult to differentiate between the substrate and the coating, which implies that a good interface coating-substrate and good epoxy–epoxy (coating-substrate) compatibility were achieved.

To analyze the electrical conductivity of the coated substrates, a test was performed in two ranges from 0 to 20 V and from 0 to 100 V applying current limits of 1 and 0.02 A, respectively. The coatings present a dimension of 100 × 50 (W × L), so the distance between electrodes was 50 mm (Figure 7b). Linear trends were observed to have a regression coefficient of 0.99 in both cases, so the results were easily adjusted to Ohm's law (eq 2). Similar conductivity values were achieved in both analyzed ranges, 0.28 and 0.31 s·m⁻¹ for 0–

20 and 0–100 V, respectively. It can be noted that lower values were obtained with the coating than the bulks samples for the same CF content (12.5%), this difference can result from the difficulty of obtaining a homogeneous distribution of the fibers throughout the volume of the matrix by applying a coating, which can be more easily obtained by pouring the matrix (as in the bulk manufacturing). Additionally, due to the large difference in the surface area between the bulk samples and the coatings, it is more likely to find a region with a different CF content or thickness, which can significantly affect the overall conductivity of the tested sample.

The Joule effect is also studied on the coating (Figure 7b). Tests were performed at 12, 24, 48, and 100 V. In all cases, the coating area (50 cm²) was completely heated, and averages temperatures of 35, 52, 98, and 170 °C were achieved in less than 3 min. A thermal image of the experiment with 100 V is shown in Figure 7c, where it is possible to observe the global heating of the coating, after 120 s, with some areas at temperatures above 170 °C. Finally, to determine if the Joule effect heating can influence the adhesion of the coating, pull-off adhesion tests were carried out on coatings before and after carrying out the Joule effect heating tests. In this way it was possible to observe how the heating cycle did not significantly affect the adhesion of the coating, obtaining a result of 9.36 ± 0.14 and 9.73 ± 0.48 MPa, before and after the Joule effect heating, respectively.

4. CONCLUSIONS

In the present investigation, expired CF prepreg waste tapes were milled, generating recycled short CFs, in the range of 50–200 μm, which were added into an epoxy resin to produce a novel multifunctional coating and bulk material as a waste management alternative to the CFRP industry. Contents up to 12.5 wt % were added to an epoxy matrix as higher contents were not processable due to the high viscosity and low wettability of the CF, even though sonication and surfactant addition were used to improve the dispersion and distribution through the matrix. The number of milling cycles not only has an effect in the reduction of the average length but also helps to reduce the amount of resin from the prepreg waste as proved by TGA analysis.

Excellent results were achieved on the electrical conductivity test obtaining values from 0.33 to 2.1 S·m⁻¹, results far superior to those observed in the literature for other carbon reinforcements, such as graphene or nanotubes, in epoxy resins. Regarding the Joule effect heating, high temperatures were achieved quickly in all cases, despite low voltages being used to perform the experiments (12, 24, and 48 V). Best results were obtained in the case of using 48 V, where a temperature of 200 °C was achieved in less than 17 s with all samples.

These excellent properties of these multifunctional materials, as bulk or coating, assess their huge potential as a high added value for the recycled products in different applications, which in turn would avoid the use of nanoparticles as the values obtained are in the same value or above those reached by CNT or GNP reinforced epoxy coatings.

AUTHOR INFORMATION

Corresponding Authors

David Martinez-Diaz – Materials Science and Engineering Area, Rey Juan Carlos University, Móstoles 28933, Spain;

orcid.org/0000-0003-2320-8552;

Email: david.martinez.diaz@urjc.es

Silvia González Prolongo – Materials Science and Engineering Area, Rey Juan Carlos University, Móstoles 28933, Spain; orcid.org/0000-0002-4438-6123; Email: silvia.gonzalez@urjc.es

Authors

Emma Espeute – Materials Science and Engineering Area, Rey Juan Carlos University, Móstoles 28933, Spain; Centrale Lille Institut—École Nationale Supérieure de Chimie de Lille, ENSCL, Villeneuve-d'Ascq 59651, France

Alberto Jiménez-Suárez – Materials Science and Engineering Area, Rey Juan Carlos University, Móstoles 28933, Spain; orcid.org/0000-0001-8416-6398

Complete contact information is available at:

<https://pubs.acs.org/10.1021/acsomega.3c05413>

Author Contributions

All authors contributed equally to this work.

Notes

The authors declare no competing financial interest.

ACKNOWLEDGMENTS

This work was supported by the Agencia Estatal de Investigación of Spanish Government by the projects TED2021-131102B-C21 and PID2022-138496OB-I00, and by AIRBUS OPERATIONS SL with the project WING-EOL SELF-HEALING COATING.

REFERENCES

- (1) Zhao, Q.; An, L.; Li, C.; Zhang, L.; Jiang, J.; Li, Y. Environment-Friendly Recycling of CFRP Composites via Gentle Solvent System at Atmospheric Pressure. *Compos. Sci. Technol.* **2022**, *224*, 109461.
- (2) Borjan, D.; Knez, Z.; Knez, M. Recycling of Carbon Fiber-Reinforced Composites— Difficulties and Future Perspectives. *Materials*; MDPI AG, 2021. August 1.
- (3) Meshoyrer, E.; Pan, C.; Yao, B.; Zhang, J.; Chang, E. Development of Polymer Composites Reinforced with Recycled Carbon Fibers. *2019 IEEE MIT Undergraduate Research Technology Conference, URTC 2019*; Institute of Electrical and Electronics Engineers Inc., 2019.
- (4) Zhang, J.; Lin, G.; Vaidya, U.; Wang, H. Past, Present and Future Prospective of Global Carbon Fibre Composite Developments and Applications. *Composites, Part B* **2023**, *250*, 110463.
- (5) Trivyza, N. L.; Rentizelas, A.; Oswald, S.; Siegl, S. Designing Reverse Supply Networks for Carbon Fibres: Enabling Cross-Sectoral Circular Economy Pathways. *J. Cleaner Prod.* **2022**, *372*, 133599.
- (6) Lunetto, V.; Galati, M.; Settineri, L.; Iuliano, L. Sustainability in the Manufacturing of Composite Materials: A Literature Review and Directions for Future Research. *J. Manuf. Process.* **2023**, *85*, 858–874.
- (7) Gharfalkar, M.; Court, R.; Campbell, C.; Ali, Z.; Hillier, G. Analysis of Waste Hierarchy in the European Waste Directive 2008/98/EC. *Waste Manage.* **2015**, *39*, 305–313.
- (8) Groetsch, T.; Maghe, M.; Creighton, C.; Varley, R. J. Environmental, Property and Cost Impact Analysis of Carbon Fibre at Increasing Rates of Production. *J. Cleaner Prod.* **2023**, *382*, 135292.
- (9) Bianchi, I.; Forcellese, A.; Marconi, M.; Simoncini, M.; Vita, A.; Castorani, V. Environmental Impact Assessment of Zero Waste Approach for Carbon Fiber Prepreg Scraps. *Sustainable Mater. Technol.* **2021**, *29*, No. e00308.
- (10) Pakdel, E.; Kashi, S.; Baum, T.; Usman, K. A. S.; Razal, J. M.; Varley, R.; Wang, X. Carbon Fibre Waste Recycling into Hybrid Nonwovens for Electromagnetic Interference Shielding and Sound Absorption. *J. Cleaner Prod.* **2021**, *315*, 128196.

- (11) Chen, C. H.; Chiang, C. L.; Wang, J. X.; Shen, M. Y. A Circular Economy Study on the Characterization and Thermal Properties of Thermoplastic Composite Created Using Regenerated Carbon Fiber Recycled from Waste Thermoset CFRP Bicycle Part as Reinforcement. *Compos. Sci. Technol.* **2022**, *230*, 109761.
- (12) Directive, E. C. *Directive 2008/98/EC of the European Parliament and of the Council of 19 November 2008 on Waste and Repealing Certain Directives*; Official Journal of the European Union, 2018.
- (13) Nilakantan, G.; Nutt, S. Reuse and Upcycling of Aerospace Prepreg Scrap and Waste. *Reinf. Plast.* **2015**, *59* (1), 44–51.
- (14) Chadwick, C.; Kalaitzidou, K.; Colton, J. Processing of Post-Industrial Unidirectional Prepreg Tapes Using SMC Equipment. *Int. J. Adv. Manuf. Technol.* **2022**, *121* (3–4), 2831–2839.
- (15) Vita, A.; Forcellese, A.; Simoncini, M. Reuse of Composite Prepreg Scraps as an Economic and Sustainable Alternative for Producing Car Components. In *Selected Topics in Manufacturing: AITeM Young Researcher Award 2021*; Carrino, L., Tolio, T., Eds.; Springer International Publishing: Cham, 2022; pp 171–188.
- (16) Sultana, S.; Asadi, A.; Colton, J.; Kalaitzidou, K. Composites Made from CF Prepreg Trim Waste Tapes Using Sheet Molding Compounds (SMC) Technology: Challenges and Potential. *Composites, Part A* **2020**, *134*, 105906.
- (17) Oliveux, G.; Dandy, L. O.; Leeke, G. A. Current Status of Recycling of Fibre Reinforced Polymers: Review of Technologies, Reuse and Resulting Properties. *Progress in Materials Science*; Elsevier Ltd, 2015; pp 61–99. July 1.
- (18) Martínez-Díaz, D.; Cortés, A.; Jiménez-Suárez, A.; Prolongo, S. G. Hardener Isomerism and Content of Dynamic Disulfide Bond Effect on Chemical Recycling of Epoxy Networks. *ACS Appl. Polym. Mater.* **2022**, *4* (7), 5068–5076.
- (19) Knappich, F.; Klotz, M.; Schlummer, M.; Wölling, J.; Mäurer, A. Recycling Process for Carbon Fiber Reinforced Plastics with Polyamide 6, Polyurethane and Epoxy Matrix by Gentle Solvent Treatment. *Waste Manage.* **2019**, *85*, 73–81.
- (20) Lee, M.; Kim, D. H.; Park, J. J.; You, N. H.; Goh, M. Fast Chemical Recycling of Carbon Fiber Reinforced Plastic at Ambient Pressure Using an Aqueous Solvent Accelerated by a Surfactant. *Waste Manage.* **2020**, *118*, 190–196.
- (21) Cheng, H.; Guo, L.; Zheng, L.; Qian, Z.; Su, S. A Closed-Loop Recycling Process for Carbon Fiber-Reinforced Polymer Waste Using Thermally Activated Oxide Semiconductors: Carbon Fiber Recycling, Characterization and Life Cycle Assessment. *Waste Manage.* **2022**, *153*, 283–292.
- (22) Lopez-Urionabarrenechea, A.; Gastelu, N.; Acha, E.; Caballero, B. M.; de Marco, I. Production of Hydrogen-Rich Gases in the Recycling Process of Residual Carbon Fiber Reinforced Polymers by Pyrolysis. *Waste Manage.* **2021**, *128*, 73–82.
- (23) Sommer, V.; Walther, G. Recycling and Recovery Infrastructures for Glass and Carbon Fiber Reinforced Plastic Waste from Wind Energy Industry: A European Case Study. *Waste Manage.* **2021**, *121*, 265–275.
- (24) Shuaib, N. A.; Mativenga, P. T. Energy Demand in Mechanical Recycling of Glass Fibre Reinforced Thermoset Plastic Composites. *J. Cleaner Prod.* **2016**, *120*, 198–206.
- (25) Liu, Y.; Farnsworth, M.; Tiwari, A. A Review of Optimisation Techniques Used in the Composite Recycling Area: State-of-the-Art and Steps towards a Research Agenda. *J. Cleaner Prod.* **2017**, *140*, 1775–1781.
- (26) Cheng, H.; Zhou, J.; Guo, L.; Wang, H.; Qian, Z. Dispersibility Optimization of Short Carbon Fiber Suspension for the Preparation of Carbon Fiber Aligned Mat Reinforced Composites. *J. Cleaner Prod.* **2023**, *389*, 136075.
- (27) Quan, D.; Liu, J.; Yao, L.; Dransfeld, C.; Alderliesten, R.; Zhao, G. Interlaminar and Intralaminar Fracture Resistance of Recycled Carbon Fibre/PPS Composites with Tailored Fibre/Matrix Adhesion. *Compos. Sci. Technol.* **2023**, *239*, 110051.
- (28) Lendlein, A.; Trask, R. S. Multifunctional Materials: Concepts, Function-Structure Relationships, Knowledge-Based Design, Translational Materials Research. *Multifunctional Materials*; IOP Publishing Ltd, 2018. December 1.
- (29) He, Z.; Wang, J. Anti-Icing Strategies Are on the Way. *The Innovation*; Cell Press, 2022. September 13.
- (30) Redondo, O.; Prolongo, S. G.; Campo, M.; Sbarufatti, C.; Giglio, M. Anti-Icing and de-Icing Coatings Based Joule's Heating of Graphene Nanoplatelets. *Compos. Sci. Technol.* **2018**, *164*, 65–73.
- (31) Prolongo, S. G.; Moriche, R.; Del Rosario, G.; Jiménez-Suárez, A.; Prolongo, M. G.; Ureña, A. Joule Effect Self-Heating of Epoxy Composites Reinforced with Graphitic Nanofillers. *J. Polym. Res.* **2016**, *23*, 189.
- (32) Sun, J.; Li, X.; Tian, X.; Chen, J.; Yao, X. Dynamic Electrical Characteristics of Carbon Fiber-Reinforced Polymer Composite under Low Intensity Lightning Current Impulse. *Advanced Composites Letters* **2020**, *29*, 2633366X2094277.
- (33) Sánchez-Romate, X. F.; González, C.; Jiménez-Suárez, A.; Prolongo, S. G. Novel Approach for Damage Detection in Multiscale CNT-Reinforced Composites via Wireless Joule Heating Monitoring. *Compos. Sci. Technol.* **2022**, *227*, 109614.
- (34) Sangroniz, L.; Landa, M.; Fernández, M.; Santamaria, A. Matching Rheology, Conductivity and Joule Effect in PU/CNT Nanocomposites. *Polymers (Basel)* **2021**, *13* (6), 950.
- (35) Sánchez-Romate, X. F.; Sans, A.; Jiménez-Suárez, A.; Campo, M.; Ureña, A.; Prolongo, S. G. Highly Multifunctional GNP/Epoxy Nanocomposites: From Strain-Sensing to Joule Heating Applications. *Nanomaterials* **2020**, *10* (12), 2431.
- (36) Zhao, Y.; Liu, H.; Li, S.; Chen, P.; Jiang, S.; Liu, J.; Meng, F. Rapid Joule-Heating Activation Boosted Capacitive Performance of Carbon Fibers. *Compos. Commun.* **2022**, *34*, 101263.
- (37) Logesh, G.; Srishilan, C.; Sabu, U.; Prasad, K.; Rashad, M.; Joseph, A.; James Raju, K. C.; Balasubramanian, M. Carbon Fiber Reinforced Composites from Industrial Waste for Microwave Absorption and Electromagnetic Interference Shielding Applications. *Ceram. Int.* **2023**, *49*, 1922–1931.
- (38) Wang, W.; Lu, H.; Lu, Z.; Qian, C.; Shen, L.; Long, Z.; Xu, H.; Dong, Y. Development of Electrothermal-Driven Graphene Fiber/Carbon Fiber/Poly (Ethylene-Co-Vinyl Acetate) Shape Memory Composites for Electromagnetic Shielding. *Mater. Lett.* **2022**, *328*, 133114.
- (39) Wang, B.; Ming, Y.; Zhu, Y.; Yao, X.; Ziegmann, G.; Xiao, H.; Zhang, X.; Zhang, J.; Duan, Y.; Sun, J. Fabrication of Continuous Carbon Fiber Mesh for Lightning Protection of Large-Scale Wind-Turbine Blade by Electron Beam Cured Printing. *Addit. Manuf.* **2020**, *31*, 100967.
- (40) Zhu, H.; Fu, K.; Liu, H.; Yang, B.; Chen, Y.; Kuang, C.; Li, Y. Design a Dual-Layer Lightning Strike Protection for Carbon Fiber Reinforced Composites. *Composites, Part B* **2022**, *247*, 110330.
- (41) Bhardwaj, P.; Grace, A. N. Antistatic and Microwave Shielding Performance of Polythiophene-Graphene Grafted 3-Dimensional Carbon Fibre Composite. *Diam. Relat. Mater.* **2020**, *106*, 107871.
- (42) Lin, T.; Jia, D.; He, P.; Wang, M.; Liang, D. Effects of Fiber Length on Mechanical Properties and Fracture Behavior of Short Carbon Fiber Reinforced Geopolymer Matrix Composites. *Mater. Sci. Eng. A* **2008**, *497* (1–2), 181–185.
- (43) de Monte, M.; Moosbrugger, E.; Jaschek, K.; Quaresimin, M. Multiaxial Fatigue of a Short Glass Fibre Reinforced Polyamide 6.6 - Fatigue and Fracture Behaviour. *Int. J. Fatigue* **2010**, *32* (1), 17–28.
- (44) Wan, Y. J.; Tang, L. C.; Gong, L. X.; Yan, D.; Li, Y. B.; Wu, L. B.; Jiang, J. X.; Lai, G. Q. Grafting of Epoxy Chains onto Graphene Oxide for Epoxy Composites with Improved Mechanical and Thermal Properties. *Carbon N Y* **2014**, *69*, 467–480.
- (45) Chen, H.; Chen, Z.; Mao, M.; Wu, Y.; Yang, F.; Gong, L.; Zhao, L.; Cao, C.; Song, P.; Gao, J.; Zhang, G.; Shi, Y.; Cao, K.; Tang, L. Self-Adhesive Polydimethylsiloxane Foam Materials Decorated with MXene/Cellulose Nanofiber Interconnected Network for Versatile Functionalities. *Adv. Funct. Mater.* **2023**, 2304927.
- (46) Saw, L. N.; Mariatti, M.; Azura, A. R.; Aziz, A.; Kim, J. K. Transparent, Electrically Conductive, and Flexible Films Made from

Multiwalled Carbon Nanotube/Epoxy Composites. *Composites, Part B* **2012**, *43* (8), 2973–2979.

(47) Vahedi, F.; Shahverdi, H. R.; Shokrieh, M. M.; Esmkhani, M. Effects of Carbon Nanotube Content on the Mechanical and Electrical Properties of Epoxy-Based Composites. *Xinxing Tan Cailiao/New Carbon Materials* **2014**, *29* (6), 419–425.

(48) Fogel, M.; Parlevliet, P.; Geistbeck, M.; Olivier, P.; Dantras, É. Thermal, Rheological and Electrical Analysis of MWCNTs/Epoxy Matrices. *Compos. Sci. Technol.* **2015**, *110*, 118–125.

(49) Chen, J.; Han, J.; Xu, D. Thermal and Electrical Properties of the Epoxy Nanocomposites Reinforced with Purified Carbon Nanotubes. *Mater. Lett.* **2019**, *246*, 20–23.

(50) Imran, K. A.; Shivakumar, K. N. Enhancement of Electrical Conductivity of Epoxy Using Graphene and Determination of Their Thermo-Mechanical Properties. *J. Reinf. Plast. Compos.* **2018**, *37* (2), 118–133.

(51) El-Tantawy, F.; Kamada, K.; Ohnabe, H. In Situ Network Structure, Electrical and Thermal Properties of Conductive Epoxy Resin-Carbon Black Composites for Electrical Heater Applications. *Mater. Lett.* **2002**, *56*, 112–126.

(52) Wu, T. H.; Foyet, A.; Kodentsov, A.; van der Ven, L. G. J.; van Benthem, R. A. T. M.; de With, G. Curing and Percolation for Carbon Black-Epoxy-Amine Nanocomposites. *Compos. Sci. Technol.* **2019**, *181*, 107672.

(53) Tsotra, P.; Friedrich, K. Short Carbon Fiber Reinforced Epoxy Resin/Polyaniline Blends: Their Electrical and Mechanical Properties. *Compos. Sci. Technol.* **2004**, *64* (15), 2385–2391.

(54) Yao, R.; Liu, X.; Jiang, W.; Shang, N.; Zheng, J.; Drechsler, K.; Shi, J. Simulation Studies Underlying the Influence of Filler Orientation on the Electrical Properties of Short Carbon Fiber Conductive Polymer Composites: Implications for Electrical Conductivity Regulation of Micro/Nanocomposites. *ACS Appl. Nano Mater.* **2023**, *6*, 9757–9767.

(55) Farcas, C.; Galao, O.; Vertuccio, L.; Guadagno, L.; Romero-Sánchez, M. D.; Rodríguez-Pastor, I.; Garcés, P. Ice-Prevention and de-Icing Capacity of Epoxy Resin Filled with Hybrid Carbon-Nanostructured Forms: Self-Heating by Joule Effect. *Nanomaterials* **2021**, *11* (9), 2427.

(56) Sanivada, U. K.; Esteves, D.; Arruda, L. M.; Silva, C. A.; Moreira, I. P.; Figueiro, R. Joule-Heating Effect of Thin Films with Carbon-Based Nanomaterials. *Materials* **2022**, *15* (12), 4323.